THE FASEB JOURNAL • RESEARCH • www.fasebj.org

Microgravity-induced hepatogenic differentiation of rBMSCs on board the SJ-10 satellite

Dongyuan Lü,[*,†,‡] Shujin Sun,[*,†,‡] Fan Zhang,[*,†,‡] Chunhua Luo,[*,†] Lu Zheng,[*,†,‡] Yi Wu,[*,†,‡] Ning Li,[*,†,‡] Chen Zhang,[*,†] Chengzhi Wang,[*,†,‡] Qin Chen,[*,†] and Mian Long[*,†,‡,1]

[*]Key Laboratory of Microgravity, Center of Biomechanics and Bioengineering and [†]Beijing Key Laboratory of Engineered Construction and Mechanobiology, Institute of Mechanics, Chinese Academy of Sciences, Beijing, China; and [‡]School of Engineering Sciences, University of Chinese Academy of Sciences, Beijing, China

ABSTRACT: Bone marrow–derived mesenchymal stem cells (BMSCs) are able to differentiate into functional hepatocytelike cells, which are expected to serve as a potential cell source in regenerative medicine, tissue engineering, and clinical treatment of liver injury. Little is known about whether and how space microgravity is able to direct the hepatogenic differentiation of BMSCs in the actual space microenvironment. In this study, we examined the effects of space microgravity on BMSC hepatogenic differentiation on board the SJ-10 Recoverable Scientific Satellite. Rat BMSCs were cultured and induced in hepatogenic induction medium for 3 and 10 d in custom-made space cell culture hardware. Cell growth was monitored periodically in orbit, and the fixed cells and collected supernatants were retrieved back to the Earth for further analyses. Data indicated that space microgravity improves the differentiating capability of the cells by up-regulating hepatocyte-specific albumin and cytokeratin 18. The resulting cells tended to be maturated, with an in-orbit period of up to 10 d. In space, mechanosensitive molecules of β1-integrin, β-actin, α-tubulin, and Ras homolog gene family member A presented enhanced expression, whereas those of cell-surface glycoprotein CD44, intercellular adhesion molecule 1, vascular cell adhesion molecule 1, vinculin, cell division control protein 42 homolog, and Rho-associated coiled-coil kinase yielded reduced expression. Also observed in space were the depolymerization of actin filaments and the accumulation of microtubules and vimentin through the altered expression and location of focal adhesion complexes, Rho guanosine 5′-triphosphatases, as well as the enhanced exosome-mediated mRNA transfer. This work furthers the understanding of the underlying mechanisms of space microgravity in directing hepatogenic differentiation of BMSCs.—Lü, D., Sun, S., Zhang, F., Luo, C., Zheng, L., Wu, Y., Li, N., Zhang, C., Wang, C., Chen, Q., Long, M. Microgravity-induced hepatogenic differentiation of rBMSCs on board the SJ-10 satellite. FASEB J. 33, 000–000 (2019). www.fasebj.org

KEY WORDS: mesenchymal stem cells · mechanotransduction · hepatocyte · signaling pathway

The human liver is a vital organ in digestion and metabolism and supports other organs in the body. At present, liver diseases pose an important problem for human health around the world. Although liver dialysis techniques can be used for the short term, there is scarce compensation in liver function for the long term. The most effective therapeutic method for curing liver failure is organ transplantation, which is limited by the lack of liver donors, immunologic rejection, and huge cost. Cell-based approaches, including hepatocyte transplantation and tissue-engineered livers, provide potential alternatives and are expected to support the lives of patients until liver organ transplantation or recovery *via* regeneration of a damaged liver is available. However, an abundant appropriate cell source is the biggest problem in engineered liver reconstruction and liver disease treatment.

Recently, cell-based approaches using human primary hepatocytes or stem cell–derived hepatocytelike cells (HLCs) are assumed to be a therapeutic option that has attracted significant attention for the treatment of liver diseases. For example, mesenchymal stem cells (MSCs) can differentiate into many other cell types, such as osteoblasts (1), chondrocytes (2), cardiomyocytes (3), adipocytes (4), endothelial cells (5), and neuronal cells (6), which may also serve as a promising source for cell

ABBREVIATIONS: ALB, albumin; BMSC, bone marrow–derived MSC; Cdc42, cell division control protein 42 homolog; CK18, cytokeratin 18; CYP450, cytochrome P450; dH_2O, distilled water; DPBS, Dulbecco's PBS; FAK, focal adhesion kinase; GO, Gene Ontology; GTPase, guanosine 5′-triphosphatase; HLC, hepatocytelike cell; ICAM-1, intercellular adhesive molecule 1; IF, immunofluorescence; MSC, mesenchymal stem cell; rBMSC, rat BMSC; RhoA, Ras homolog gene family member A; ROCK, Rho-associated protein kinase; SCCS, space cell culture system; SEM, scanning electron microscope; VCAM-1, vascular cell adhesion molecule 1

[1] Correspondence: Institute of Mechanics, Chinese Academy of Sciences, No. 15 North 4th Ring Rd., Beijing 100190, China. E-mail: mlong@imech.ac.cn

doi: 10.1096/fj.201802075R

This article includes supplemental data. Please visit *http://www.fasebj.org* to obtain this information.

therapy of liver diseases to overcome the above shortcomings of cell accessibility and abundance. In fact, MSCs can differentiate into hepatogenic parenchymal cells expressing hepatic biomarkers with hepatocyte functionality (7). MSC-derived HLCs could replace human primary hepatocytes in drug discovery and hepatotoxic tests (8–10). However, the generation of fully functional HLCs is still a big challenge, and plenty of work has been focusing on improving the existing differentiation protocols to achieve mature HLCs with hepatocellular morphology and function. Producing abundant functional HLCs from MSCs is also of great urgency for applying bio-artificial liver support systems and hepatocyte-based therapy.

MSCs are a kind of typical mechanosensitive cell, and mechanical responses in MSCs guide both differentiation and function, mainly depending on the specific physical and mechanical microenvironment around the cells. Growing evidence shows that physical features and mechanical stresses, independent of soluble biochemical factors, help determine MSCs' fate, indicating that mechanical factors are favorable inducers for stem cells' application in clinical treatment. Specifically in space, the microgravity, as a mechanical factor, regulates both differentiation and function of MSCs to different cell types and increases cellular activity (11). MSCs are exemplified as angiogenesis (11), osteogenesis (12, 13), chondrogenesis (14), and formation of neural cells and adipocytes (15) by ground-based commercial devices such as clinostats (12), rotary cell culture systems (14), random position machines (11), and rotating wall vessel bioreactors (13); by customer-made microgravity effect simulators (16); or by the real microgravity environment in space (17). However, the effects of space microgravity on hepatogenic differentiation potentials of bone marrow–derived MSCs (BMSCs) are still unclear, mainly because of few ground-based microgravity effect studies (18) and the lack of those space microgravity–based works.

It is well known that modified gravity not only affects the organism as a whole but also modulates the molecular processes in individual cells (19, 20). We proposed that gravity could influence the hepatogenic differentiation of MSCs. To prove this hypothesis, here the effects of space microgravity were tested on cellular phenotype, hepatogenic differentiation, and altered expression of the underlying mechanotransductive molecules of rat BMSCs (rBMSCs) cultured on board the SJ-10 Recoverable Scientific Satellite. Producing MSC-derived differentiated cells with primary hepatic functions in microgravity could provide new insights in collecting functional hepatocytes on the ground for treating end-stage liver patients, and it could also be useful for other biomedical applications, such as drug screening.

MATERIALS AND METHODS

Cells and reagents

This study was performed in accordance with standard ethics guidelines and approved by the Ethics Committee of the Institute of Mechanics, Chinese Academy of China. rBMSCs were isolated from their bone marrow, as previously described (21). In brief, rBMSCs were isolated from 3- to 4-wk-old male Sprague-Dawley rats (Vital River Laboratory Animal Technology, Beijing, China). The animals were euthanized by cervical dislocation and sterilized with alcohol, and then the femur and tibia were collected. The bone marrow was flushed out, and the collected cell suspension was added to DMEM/F12 medium supplemented with 15% fetal bovine serum and 1% nonessential amino acid (v/v), 1% glutamine (v/v), 1% sodium pyruvate (v/v), and 1% penicillin/streptomycin (v/v) in a T-25 flask; all the reagents were purchased from Thermo Fisher Scientific (Waltham, MA, USA) and used per the manufacturer's instructions. Adherent cells were then maintained in a humidified, 37°C incubator with 95% air and 5% carbon dioxide, 37°C incubator by refreshing the medium every 2 or 3 d. When grown up to 85–90% confluence, the cells were rinsed in Ca^{2+} and Mg^{2+}-free PBS and then detached using 0.25% trypsin-EDTA for about 1 min. This procedure was repeated 3 or 4 times to collect rBMSCs at ~90% purity. Goat anti-rat anti-CD11b, -CD34, -CD45, and -CD90 mAbs were purchased from Santa Cruz Biotechnology (Dallas, TX, USA) and used as MSCs' biomarkers (21).

Hepatogenic differentiation of rBMSCs

The standard hepatogenic differentiation protocol for MSCs (22) was modified to adapt the spaceflight mission of the SJ-10 satellite. Briefly, rBMSCs at passage 4 were cultured in rBMSC culture medium supplemented with 20 ng/ml hepatocyte growth factor and 10 ng/ml epidermal growth factor for 10 d. The medium was exchanged every 3 d prior to the mission. All the reagents were purchased from R&D Systems (Minneapolis, MN, USA).

Cell culture hardware and spaceflight mission

The spaceflight experiment was performed in a space cell culture system (SCCS) built in-house (Supplemental Fig. S1*A*, *B*) by the National Microgravity Laboratory, Institute of Mechanics, Chinese Academy of Sciences. This device was mounted in the SJ-10 satellite launched on April 6 and recovered on April 18, 2016 (Supplemental Fig. S1*C*) (23, 24). At 36 h before launch, 2 cell culture chambers with an effective culture area of 12 cm^2 each were filled with a cell suspension containing 5×10^5 rBMSCs per chamber and placed in an incubator for 12 h at 37°C to allow cell attachment. At 19 h prior to launch, the 2 chambers were refilled with fresh hepatogenic induction medium to wash out the unattached cells and to eliminate air bubbles and then mounted in the SCCS. The SCCS was inflated by premixed 95% air and 5% CO_2, sealed at 1 atm, and assembled onto the platform of the SJ-10 satellite at 8 h prelaunch. Gas exchange between the medium and the environment in the SCCS was available through a silicon rubber seal of the culture chamber and connected silicon rubber tubes. The cells in the 2 chambers were maintained at a temperature of 36 ± 1.5°C and fixed with 4% paraformaldehyde in orbit at d 3 or 10 postlaunch, respectively. The d 3 and 10 culture groups were in separate medium changing channels and pump valves. The medium for the sample fixed at d 10 was refreshed every 48 h before fixation but not refreshed for the sample fixed at d 3, and the supernatants in the 2 chambers were collected separately and preserved at 5–15°C. A total of 12 ml of supernatant was obtained for rBMSCs cultured for 10 d. All the operations in orbit were performed automatically by a set of peristaltic pumps and pinch valves controlled by a preset program. After running in orbit for 12 d, the satellite was returned to the ground. The culture chambers with fixed cells and medium samples were taken out from the SCCS and transported at 4–10°C to the laboratory in Beijing within 18 h. The culture substrates (Permanox slide, 25 × 75 mm; Nunc, Roskilde, Denmark) were disassembled from the chambers and washed 3 times with Dulbecco's PBS (DPBS), and the supernatants were stored at −80°C immediately until testing.

The corresponding ground control experiments were conducted using the same SCCS device and with identical space procedures.

Optical and scanning electron microscope imaging

The original rBMSCs and the differentiated cells placed on the culture substrate were observed by an Olympus inverted microscope (CKX41; Thermo Fisher Scientific) and recorded with a charge-coupled device camera. Each substrate was then cut into pieces and used for scanning electron microscope (SEM) imaging or immunofluorescence (IF) staining. The SEM imaging was conducted as previously described (24). In short, 1 aliquot of the samples was dehydrated with ethanol from 50–70–80–90–100% for 5 min at each gradient, transferred to *tert*-butyl alcohol twice, dried at the critical point, coated with a thin layer of gold, and finally imaged by an FEI Quanta 200 SEM (Thermo Fisher Scientific).

Antibodies and IF staining

Alexa Fluor 647–conjugated mouse anti–intercellular adhesive molecule 1 (ICAM-1) (HCD54) mAbs were obtained from BioLegend (San Diego, CA, USA). Alexa Fluor 594–conjugated rabbit anti–β-actin (13E5), Alexa Fluor 555–conjugated rabbit anti–α-tubulin (11H10), and Alexa Fluor 647–conjugated rabbit anti-vimentin (D21H3) mAbs and rabbit anti–phospho (p)-lamin A/C (D2B2E) and mouse anti–lamin A/C (4C11) mAbs were purchased from Cell Signaling Technology (Danvers, MA, USA). All other antibodies were from Abcam (Cambridge, United Kingdom), including rabbit anti-CD34 (EP373Y), anti-albumin (ALB) (C-terminal), anti–cytochrome P450 (CYP450) [EPR14479(B)], anti–acetylated histone H2B, anti–cofilin-2, anti–ERK1/2 (E337), anti-Src protein (Y232), and anti-JNK (EPR5693) mAbs; Alexa Fluor 647–conjugated rabbit anti–vascular cell adhesion molecule 1 (VCAM-1) (EPR5047), anti–cytokeratin 18 (CK18) (E431-1), anti–NF-κB (E379), anti-protein kinase B (also known as Akt) (EP2109Y), anti-vinculin (EPR8185), anti–Rho-associated protein kinase (ROCK)-1 (EP786Y), and anti–caveolin-1 (E249) mAbs; mouse anti–β1-integrin (12G10), anti-Ras-related C3 botulinum toxin substrate 1 (Rac-1) (0.T.127), anti-p–focal adhesion kinase (FAK) (Tyr^{397}, M121), anti-Ras homolog gene family, member A (RhoA) (1B12), and anti–PI3K-p85 (M253) mAbs; Alexa Fluor 488–conjugated anti–histone H2B (mAbcam 52484), Alexa Fluor 647–conjugated anti–β-catenin (EPR5047), and phycoerythrin-conjugated anti-CD44 (F10-44-2) mAbs as well as anti-Cdc42 (cell division control protein 42 homolog) polyclonal antibodies; and DyLight 594–conjugated donkey anti-rabbit and Alexa Fluor 488–conjugated goat anti-rabbit and donkey anti-mouse polyclonal secondary antibodies.

Typical mechanosensitive proteins and hepatocyte-specific biomarkers from collected rBMSCs were stained directly using the respective fluorescence-labeled antibodies. For intracellular signaling molecules, the fixed cells were permeabilized with 0.4% Triton X-100 dissolved in DPBS for 15 min and incubated successively in blocking buffer [1% bovine serum albumin (BSA) in DPBS] at 37°C for 1 h, and then primary antibodies (10 μg/ml) were diluted in 1% BSA/PBS (to block nonspecific epitopes) at 4°C overnight. The collected samples were incubated in secondary antibodies (5 μg/ml in blocking buffer) for 1 h at 37°C. After each step, the cells were washed 3 times in DPBS. At last, the samples were incubated with Hoechst 33342 for 10 min at room temperature, washed 3–5 times with PBS, and stored at 4°C. The images of stained cells were examined with a confocal laser scanning microscopy LSM 710 system (Zeiss, Oberkochen, Germany).

Oil Red O staining

After the cells were fixed using 4% paraformaldehyde and rinsed with PBS, the Oil Red O stock solution was mixed at a 6:4 ratio with distilled water (dH_2O) and left to stand for 10 min. The solution was filtered with a coffee filter or other fast filter and then added into the cells using a 0.22-μm syringe filter. The Oil Red O was incubated with the cells for 15 min and washed out with dH_2O. Collected cells were resuspended into dH_2O for microscopic imaging.

Exosome RNA profiling

A total of 10 ml of supernatant was used for exosome collection, following standard centrifugation protocols previously described (24, 25). Total RNA obtained from purified exosomes was used for library preparation and sequencing, which was performed at RiboBio (Guangzhou, China). Here, total RNA was reversely transcribed and amplified by PCR. The PCR products were sequenced using the Illumina HiSeq 3000/4000 platform (San Diego, CA, USA). Sequence data were mapped to the rat reference genome with Tophat2 (Johns Hopkins University, Baltimore, MD, USA) (26). Gene expression was quantified with values of reads per kb of transcript sequence per millions base pairs sequenced (27), and the differential expression was assessed by DEseq (28). Differentially expressed genes were chosen with the criteria of fold change >2 and $P<0.05$. Gene Ontology (GO) analysis was applied to analyze the potential functions of the differentially expressed genes using the Database for Annotation, Visualization and Integrated Discovery (29). The significance of each GO term was indicated by P value, and $P < 0.05$ was considered to be statistically significant.

Statistical analysis

Data were presented as means ± SD. The significant differences between multiple groups were analyzed by a 2-way ANOVA followed by a Holm-Šidák test. For comparisons of 2 groups, the unpaired, 2-tailed Student's t test was performed if the normality test was passed; the Mann-Whitney rank sum test was used if not. A value of $P < 0.05$ was considered statistically significant, and a value of $P < 0.01$ was considered a highly significant difference.

RESULTS

Morphology of differentiation rBMSCs

To identify whether space microgravity could affect the hepatogenic differentiation potential of rBMSCs, the modified 1-step hepatogenic differentiation protocol was applied to adapt the SJ-10 mission and the SCCS device to space, whereas the same protocols for gravity on the ground were used as a control. Morphologic changes of the cells were monitored during different stages of hepatogenic induction. At d 3, rBMSCs' growth onto a monolayer is characterized morphologically by a small cell body with a long and flat shape. The cell body contains a large, round nucleus with 1 (mostly on the ground) or 2 (merely in space) prominent nucleoli (arrows), showing a similar fibroblastlike morphology observed by an optical microscope (**Fig. 1*A*, *A′*, *B*, *B′***) and SEM (Fig. 1*C*, *C′*, *D*, *D′*). Because the appearance of dual nuclei or nucleoli is known to be one of the key features for hepatocytes (30), these observations implied that space microgravity may accelerate the initial hepatogenic differentiation as compared with normal gravity on the ground. By contrast, morphologic differences at long-term culture between the

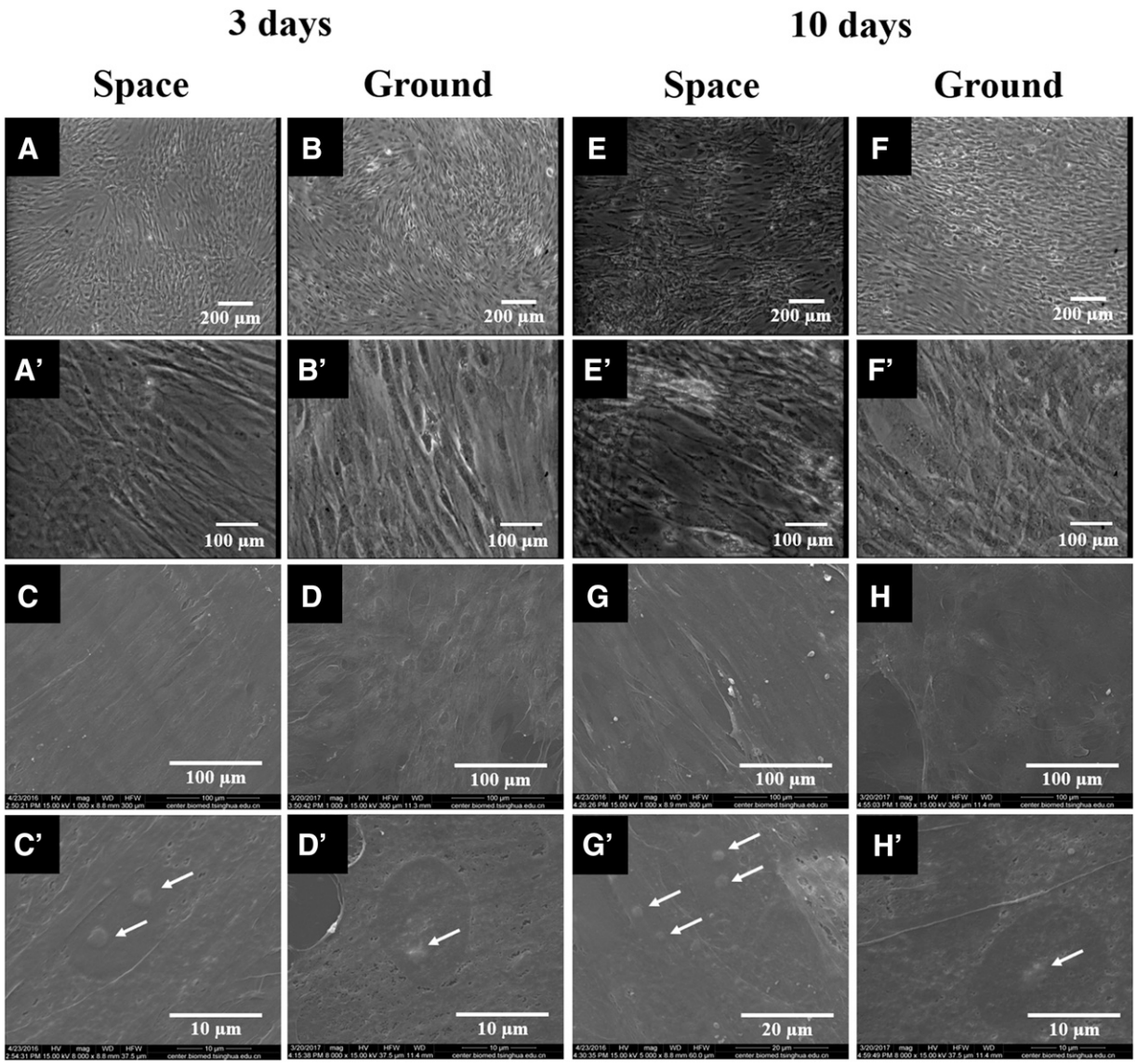

Figure 1. Morphologic representation of rBMSCs cultured in space or on the ground. Plotted are the optical (*A*, *B*, *E*, *F*) and SEM (*C*, *D*, *G*, *H*) images of rBMSCs cultured for 3 (*A–D*) or 10 (*E–H*) d in space (*A*, *C*, *E*, *G*) and on the ground (*B*, *D*, *F*, *H*). *A'–H'*) high-magnitude images of *A–H*. Arrows indicated the paired dual nuclei or nucleoli.

space sample and ground control were observed at d 10. Cells in space and ground culture also appear to form fibroblastlike morphology (Fig. 1*E*, *E'*, *F*, *F'*). A majority of cells have a single nucleus, but the hepatocytelike binucleated cells are featured commonly because many more 2-nucleoli cells can be observed in space (Fig. 1*G*, *G'*, *H*, *H'*). Intriguingly, at d 10, the cells tend to form a visible platelike structure (*i.e.*, the hepatocytes are arranged in a radial, platelike pattern) in space that does not occur with cells on the ground (Fig. 1*E*, *E'*, *F*, *F'*), suggesting the possible effects of space microgravity on directing the hepatocytelike morphology from rBMSCs that have not been observed previously. Even on 10-d hepatogenic induction, typical hepatocyte morphology with small, round, or polygonal shape was not observed yet, indicating that the differentiated cells are still immature. To determine whether the differentiated cells possess the functional characteristics of hepatocytes, the expression of typical hepatic markers was tested by IF staining at diverse differentiation points, as described below.

Characterization of rBMSC-derived HLCs

Expressions of 3 hepatocyte-specific biomarkers of ALB (**Fig. 2*A–D***), CYP450 (Fig. 2*E–H*), and CK18 (Fig. 2*I–L*) were checked for differentiating cells at d 3 (Fig. 2*A*, *C*, *E*, *G*, *I*, *K*) and d 10 (Fig. 2*B*, *D*, *F*, *H*, *J*, *L*) in space (Fig. 2*A*, *B*, *E*, *F*, *I*, *J*) and on the ground (Fig. 2*C*, *D*, *G*, *H*, *K*, *L*). Mean fluorescence intensity was estimated to compare the time dependencies and differential expression of these 3 markers for space and ground samples between d 3 and 10 (Fig. 2*M–O*). Either in space or on the ground, the expressions of ALB, CYP450, and CK18 were significantly increased from 3 to 10 d (except for a moderate increase for CYP450 on the ground), implying a time-dependent hepatogenic induction. Either at d 3 or 10, the expressions of

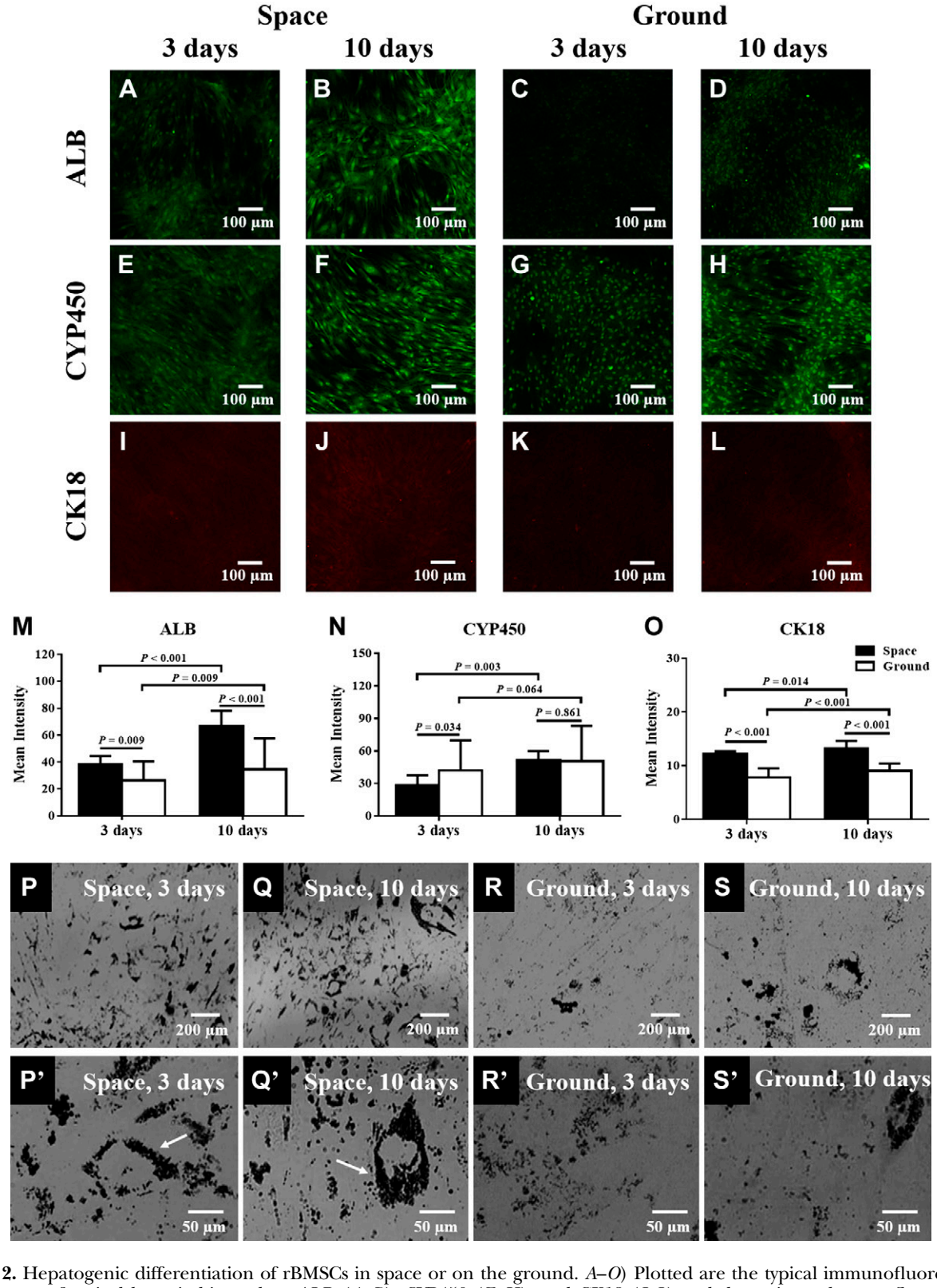

Figure 2. Hepatogenic differentiation of rBMSCs in space or on the ground. *A–O*) Plotted are the typical immunofluorescence (IF) images of typical hepatic biomarkers ALB (*A–D*), CYP450 (*E–H*), and CK18 (*I–L*) and the estimated mean fluorescence intensity of ALB (*M*), CYP450 (*N*), and CK18 (*O*) of rBMSCs cultured at d 3 or 10 in space (closed bars) and on the ground (open bars). Data are presented as the means ± SD of 20–80 images from 1 experiment in space and 3 independent experiments on the ground and were analyzed with a 2-way ANOVA followed by a Holm-Sidák test. *P–S'*) Also plotted are functional tests of differentiated rBMSCs in space or on the ground (*P–S, P'–S'*) with typical Oil Red O staining images at d 3 (*P, P', R, R'*) or d 10 (*Q, Q', S, S'*) in space (*P, P', Q, Q'*) and on the ground (*R, R', S, S'*). Arrows denote those flowerlike clusters.

ALB and CK18 were markedly up-regulated in space compared with those on the ground. At d 3, CYP450 expression was pronounced when on the ground, whereas it was moderately lower in space; at d 10, CYP450 expresison on the ground and in space was comparable. Nevertheless, these results demonstrated that the directed differentiation of rBMSCs into the cells with primary hepatic functions was likely fostered in space and gradually matured with time in the differentiation medium. Interestingly, although the differentiating cells exhibited a fibroblast-like morphology after hepatogenic induction (Fig. 2*A–L*), the expression of ALB, CYP450, or CK18 was increased with cell maturation and differentiation. These findings indicated that rBMSCs present functional potential in differentiating into cells with primary hepatic functions, especially in space microgravity.

To further test whether the differentiated cells possess mature hepatocyte function, a typical assay for lipid droplet production was conducted using Oil Red O staining of lipid vacuoles (Fig. 2*P–S*, *P′–S′*). The cells in all 4 cases were positively stained, and lipid droplets were typically arranged in flowerlike clusters in cytoplasm (*arrows*). Again, lipid droplet production was significantly increased in a time-dependent manner, with a higher production level at d 10 either in space or on the ground. Moreover, the staining was higher in cells in space than those on the ground at either d 3 (Fig. 2*P*, *P′*, *R*, *R′*) or d 10 (Fig. 2*Q*, *Q′*, *S*, *S′*), supporting the above observations of expressions of hepatic biomarkers. Collectively, the results suggested that the space environment could favor the differentiation of rBMSCs into cells with primary hepatic functions in hepatogenic induction medium.

Expression of cell adhesion molecules and focal adhesion complex proteins

Cell adhesion molecules play important roles in cell adhesion, stem cell differentiation, tissue development, and mechanotransduction. We tested 4 typical molecules of CD34, CD44, ICAM-1, and VCAM-1 (**Fig. 3**). As a specific biomarker in stem cells, CD34 was expressed in all the cases (Fig. 3*A–D*), and no time dependence between d 3 and d 10 or differential expression between space and ground samples was found (Fig. 3*Q*), except for moderate reduction on the ground from d 3 to 10. It is worth noting that CD34 distribution and characteristics were different in space and on the ground—for example, this molecule preferred to form dotlike structures over the entire cell in space (Fig. 3*A*, *B*) but not on the ground (Fig. 3*C*, *D*). By contrast, the expressions of CD44 (Fig. 3*E–H*), ICAM-1 (Fig. 3*I–L*), and

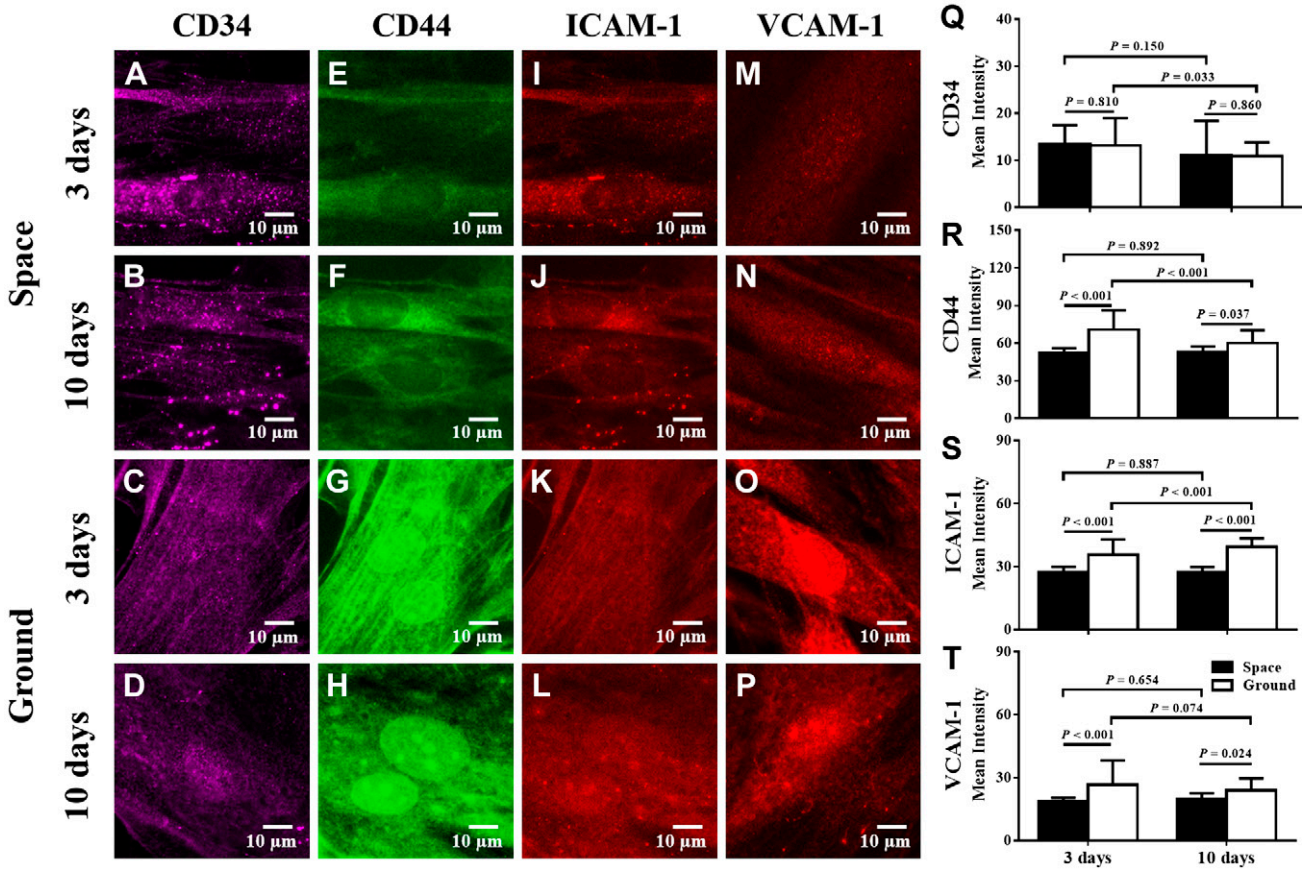

Figure 3. Effects of space microgravity on expression of cell adhesion molecules. Plotted are typical IF images (*A–P*) and estimated mean intensities (*Q–T*) of CD34 (*A–D*), CD44 (*E–H*), ICAM-1 (*I–L*), and VCAM-1 (*M–P*) on rBMSCs cultured for 3 or 10 d in space (closed bars) and on the ground (open bars). Data are presented as the means ± SD of 20–80 images from 1 experiment in space and 3 independent experiments on the ground and were analyzed with a 2-way ANOVA followed by a Holm-Šidák test.

VCAM-1 (Fig. 3*M–P*) were consistently decreased in space at either d 3 or d 10 compared with those on the ground (Fig. 3*R–T*), implying that the cell adhesion could be attenuated in space.

In fact, more important adhesive molecules for adhering MSCs onto the substrate are those in focal adhesion complexes because they are the subcellular structures that bridge cytoskeletal proteins with the extracellular matrix and mediate the mechanical forces to regulate cellular responses in space. Two typical focal adhesion proteins of β1-integrin and vinculin were thus tested (**Fig. 4**). Here, β1-integrin expression was significantly increased in space compared with that on the ground even though no difference in the expression was found between d 3 and 10 (Fig. 4*A–D*, *M*). In contrast, the trend of vinculin expression was the opposite, with higher expression on the ground than that in space at either d 3 or 10 (Fig. 4*E–H*, *N*). Because vinculin plays a key role in shape control, our data suggested that the loss of vinculin disrupts the formation of the complex, prevents cell adhesion and spreading, and inhibits lamellipodia extension. These results were consistent with the previous morphologic observations that the cells tended to be elongated but not spread out in space (Fig. 1). Taken together, these results suggest that cells in space likely became less adhesive with the progress of hepatogenic differentiation.

Cytoskeletal remodeling and mechanotransductive pathways

Induced hepatogenic differentiation of rBMSCs under space microgravity is associated with the cytoskeletal network that undergoes the mechanical support. Expressions of typical actin (**Fig. 5*A–D***), tubulin (Fig. 5*E–H*), and vimentin (Fig. 5*I–L*) in space were tested at d 3 and 10 and compared with those on the ground. Morphologically, intracellular actin stress fibers were well formed at high intensity at d 3 and weakened at d 10 in space (Fig. 5*A*, *B*), with a similar pattern to those on the ground at lower intensities (Fig. 5*C*, *D*). Particularly, the actin cytoskeleton exhibited significantly altered redistribution in space, presenting concentrated stress fibers at d 3 and sparse fibers at d 10. Such reorganization under space microgravity was presumably attributed to the coordination of biomechanical (microgravity) and biochemical (hepatocyte induction) signaling. Tubulin filaments appeared to present more visible bundles in space (Fig. 5*E*, *F*) but depicted more distinct dotted structures on the ground (Fig. 5*G*, *H*). Vimentin filaments tended to be concentrated around the nucleus in space (Fig. 5*I*, *J*) but yielded disperse distribution over the entire cell on the ground (Fig. 5*K*, *L*), as predicted previously (20, 31). Quantifying those expressions between space and ground samples, total expressions of actin (Fig. 5*M*), tubulin (Fig. 5*N*), and vimentin (Fig. 5*O*)

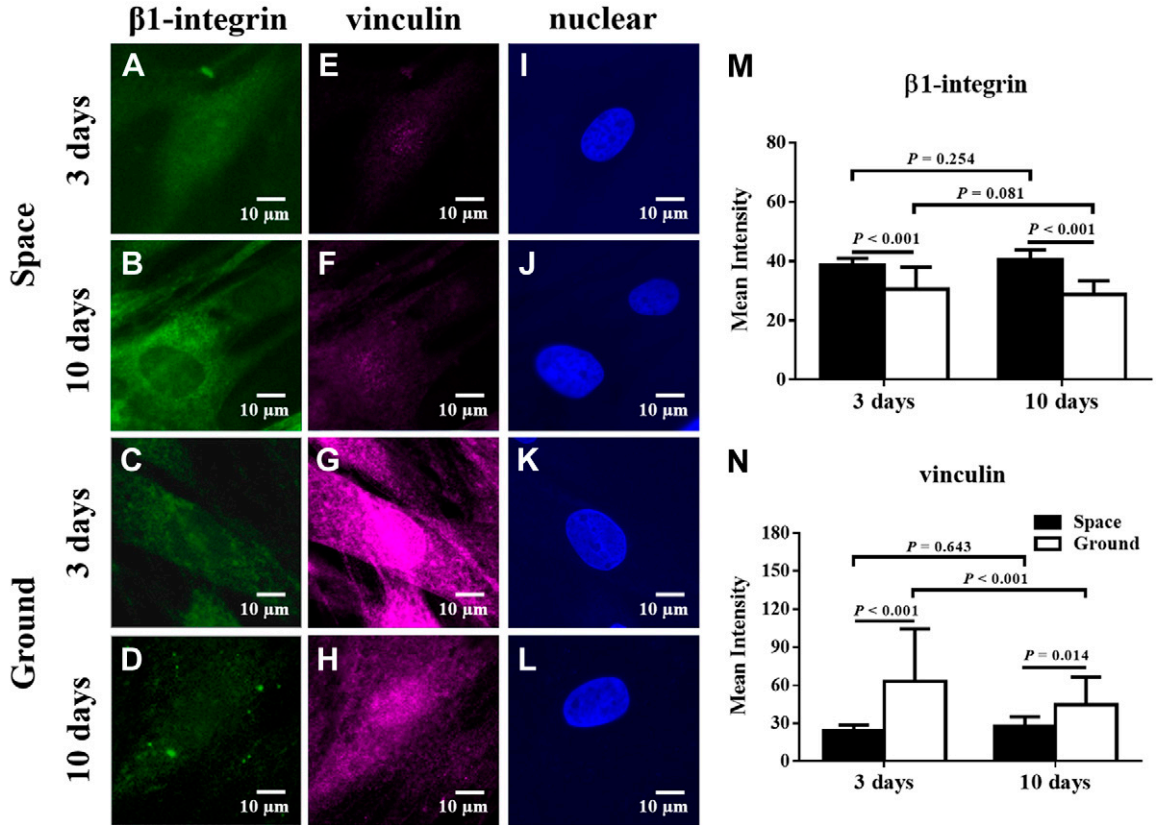

Figure 4. Effects of space microgravity on the expression of focal adhesion complex. Plotted are typical IF images (*A–L*) and estimated mean intensities (*M*, *N*) of β1-integrin (*A–D*, *M*) and vinculin (*E–H*, *N*) expressed by rBMSCs cultured for 3 or 10 d in space (closed bars) and on the ground (open bars). Cell nuclei are presented in *I–L*. Data are presented as the means ± SD of 20–80 images from 1 experiment of space sample and 3 independent experiments on the ground and were analyzed with a 2-way ANOVA followed by a Holm-Šidák test.

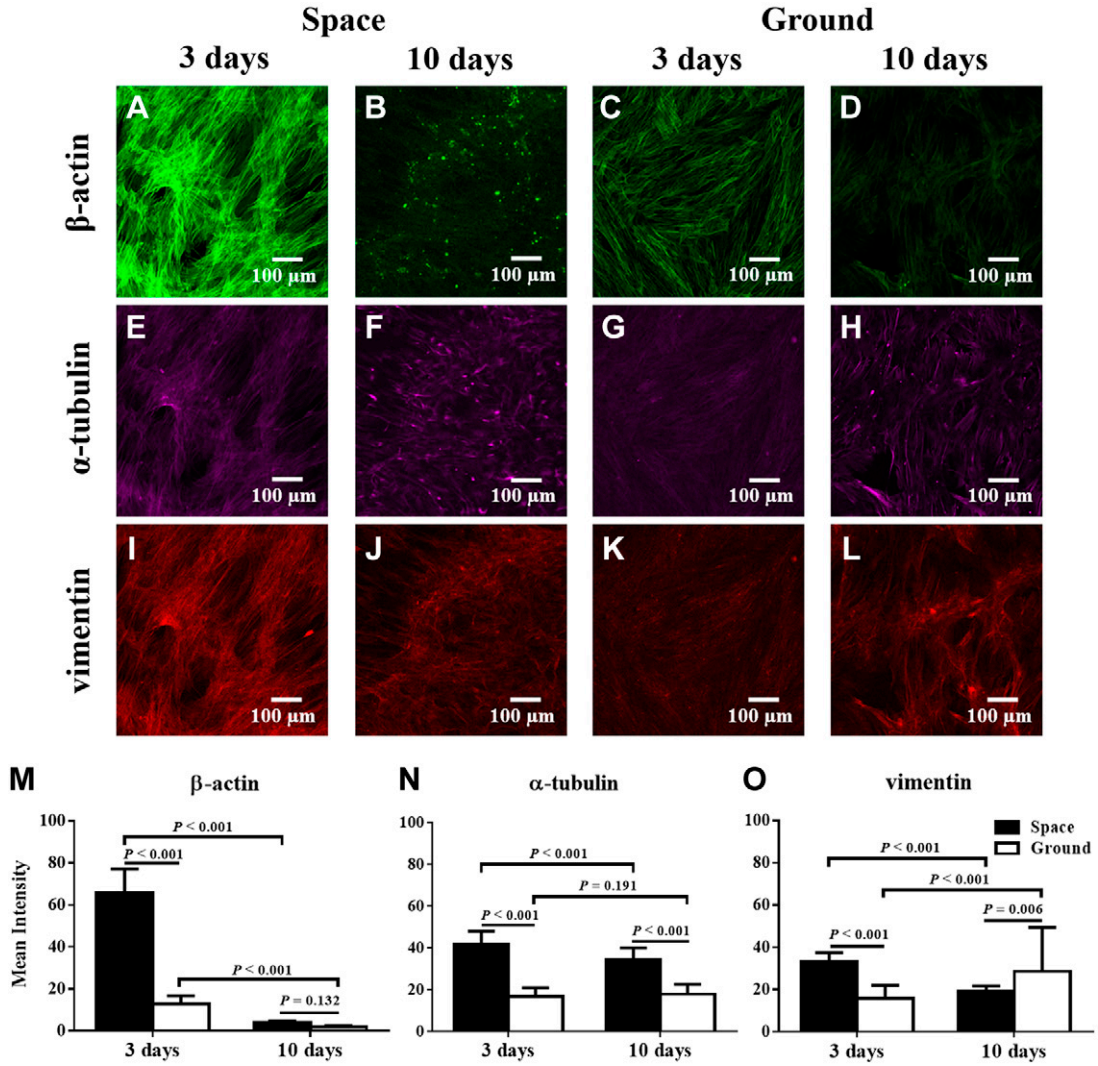

Figure 5. Effects of space microgravity on cytoskeletal remodeling. Plotted are typical IF images (*A–L*) and estimated mean intensities (*M–O*) of β-actin (*A–D*), α-tubulin (*E–H*), and vimentin (*I–L*) in rBMSCs cultured for 3 or 10 d in space (closed bars) and on the ground (open bars). Data are presented as the means ± SD of 20–80 images from 1 experiment and 3 independent experiments on the ground and were analyzed with a 2-way ANOVA followed by a Holm-Šidák test.

were surprisingly higher in space than on the ground at d 3 or 10, indicating the cytoskeletal strengthening in space for differentiating cells. By constrast, time dependence of cytoskeletal protein expression was different in space and on the ground. The expression of 3 proteins was significantly reduced from d 3 to 10 in space but was diverse on the ground, with reduced actin, comparable tubulin, and enhanced vimentin. Because the vimentin expression remained similar with tubulin at d 3 (Fig. 5*N*, *O*), the exposure to space microgravity led to a significant increase of vimentin expression at short duration. These results demonstrated that cytoskeletal remodeling outlines the underlying mechanotransduction in hepatogenic differentiation of rBMSCs in space.

To elucidate the correlation of mechanotransduction with hepatogenic differentiation signal pathways *via* cytoskeletal remodeling, the expressions of 3 typical Rho guanosine 5′-triphosphatases (GTPases) of RhoA, Rac1, and Cdc42 as well as ROCK were tested (**Fig. 6**). RhoA expression in space was comparable at d 3 or moderately enhanced at d 10 compared with that on the ground, whereas no time-dependent expression was observed either in space or on the ground (Fig. 6*A–D*, *Q*). Rac1 expression in space was comparable at d 3 or significantly reduced at d 10 compared with that on the ground, whereas time-irrelevant expression and time-dependent increase was observed for space and ground samples, respectively (Fig. 6*E–H*, *R*). Similar patterns of time dependence and differential expression were found for Cdc42 (Fig. 6*I–L*, *S*) and ROCK (Fig. 6*M–P*, *T*)—that is, the expression was sharply reduced in space at either d 3 or 10, whereas time-irrelevant expression was observed either in space or on the ground. Inserts in Fig. 6*L*, *N* illustrate the typical hepatoceullular phenotype with dual nuclei in a single differentiated cell at d 10. These diverse expressions of distinct Rho GTPases and ROCK implied that the biomechanical and biochemical cues are coupled together to regulate the complicated signaling network for rBMSC differentiation to hepatocytes in space.

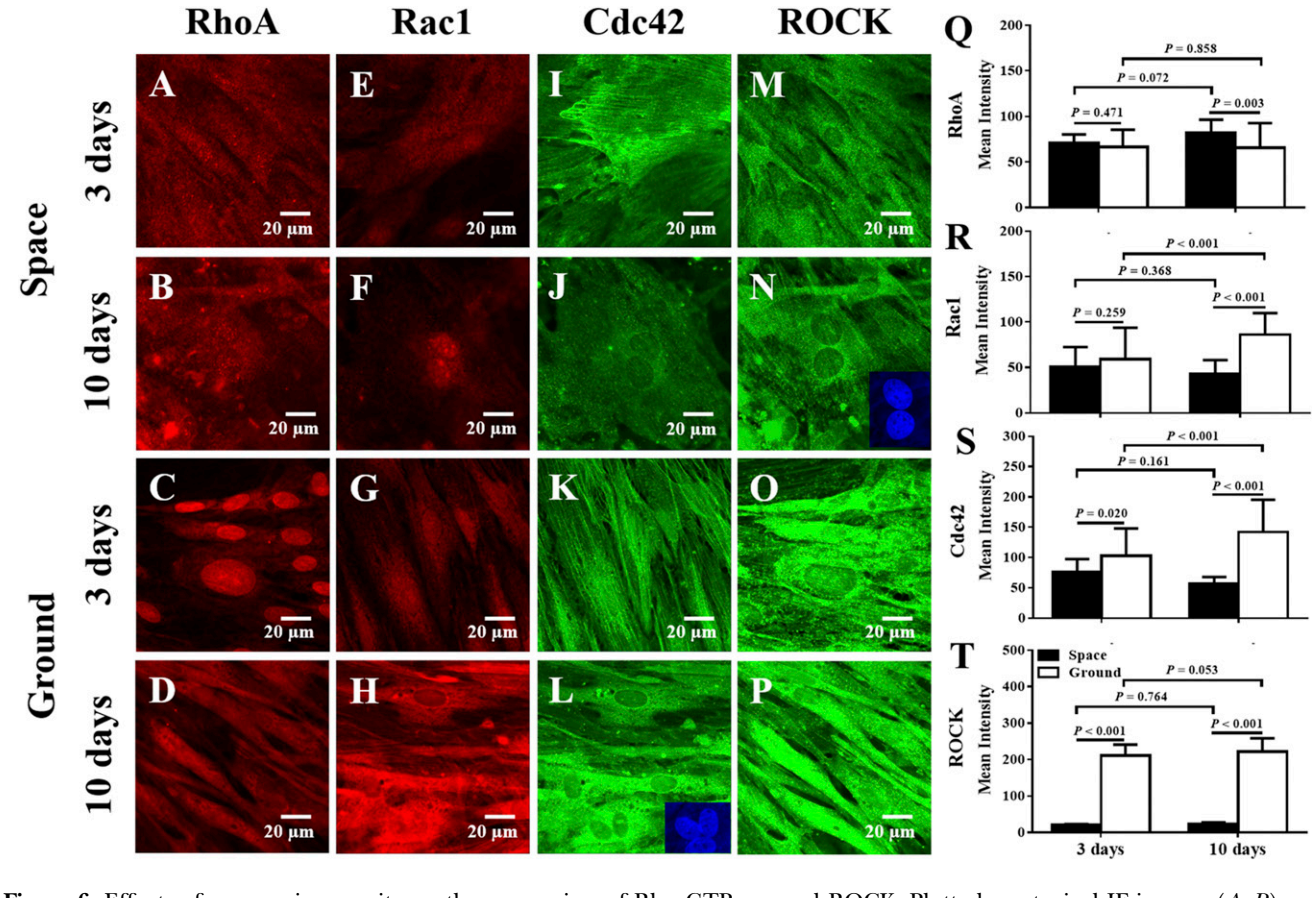

Figure 6. Effects of space microgravity on the expression of Rho GTPases and ROCK. Plotted are typical IF images (*A–P*) and measured mean intensities (*Q–T*) of RhoA (*A–D*, *Q*), Rac1 (*E–H*, *R*), Cdc42 (*I–L*, *S*), and ROCK (*M–P*, *T*) in rBMSCs cultured for 3 or 10 d in space (closed bars) and on the ground (open bars). Inserts in (*L*, *N*) illustrate the typical phenotype of dual nuclei in a single differentiated cell. Data are presented as the means ± SD of 20–80 images from 1 experiment in space and 3 independent experiments on the ground and were analyzed with a 2-way ANOVA followed by a Holm-Šidák test.

Downstream mechanotransduction under microgravity could also be associated with multiple signaling molecules, especially related to nuclear responses. Here, 3 sets of those molecules were tested systematically. Briefly, β-catenin and NF-κB expressions were increased at d 3 and 10, but FAK and Src protein expressions were decreased at d 10 in space (Supplemental Fig. S2). The expressions of cofilin-2, caveolin-1, JNK, ERK, and PI3K were likely lowered, whereas protein kinase B expression remained unchanged in space (Supplemental Fig. S3). p-lamin A/C and total H2B expressions were enhanced, but total lamin A/C and acetylated H2B were reduced in space (Supplemental Fig. S4). Diverse time dependences were also observed for distinct molecular sets. Although these results presented a complicated, time-varied signaling network, the comparisons between space and ground samples suggested that the hepatogenic differentiation of rBMSCs is, at least, mechanosensitive. For more details, refer to the Supplemental Data.

Exosome RNA profiling

Stem cells are capable of transferring genetic information to the neighboring stem cells or the stroma cells *via* the release of exosomes. To evaluate whether space microgravity can affect the exosome-mediated transfer in hepatogenic differentiation of rBMSCs, the exosomes were collected from the supernatants of rBMSCs cultured in space or on the ground separately, and the exosome RNA profile analysis was performed to investigate their roles in cell-cell communication and hepatocellular functions (**Fig. 7**). Data at d 10 were chosen to determine the possible gene expression profile in exosomes in space or on the ground. In space microgravity, 7 genes were up-regulated compared with ground controls [*i.e.*, ribosomal protein S2, ribosomal protein L14, eukaryotic translation elongation factor 1 α 1, Trns1 (also known as mt-Ts1) (tRNA), ferritin heavy chain 1, ENSRNOG00000058555 (miscellaneous RNA with unknown function), and LOC100911540 (pseudogene)]. By contrast, no down-regulated genes were found between the 2 groups (Fig. 7*A*, *B*). The differentially expressed genes play a role in gene transcription and postmodification. Typically, ribosomal protein S2 and ribosomal protein L14 are 40S- and 60S-related ribosomal proteins, respectively, constituting small and large ribosomal subunits and functioning in the posttranslational processing (32, 33). The eukaryotic translation elongation factor 1α1 protein is an isoform of the eukaryotic elongation factor 1 complex α subunit, not only being presented in both the cytoplasm for translation and in the nucleus for nuclear transport (34) but also serving as an actin bundling protein colocalized with F-actin to participate in cytoskeletal organization (35). Moreover, GO analysis was

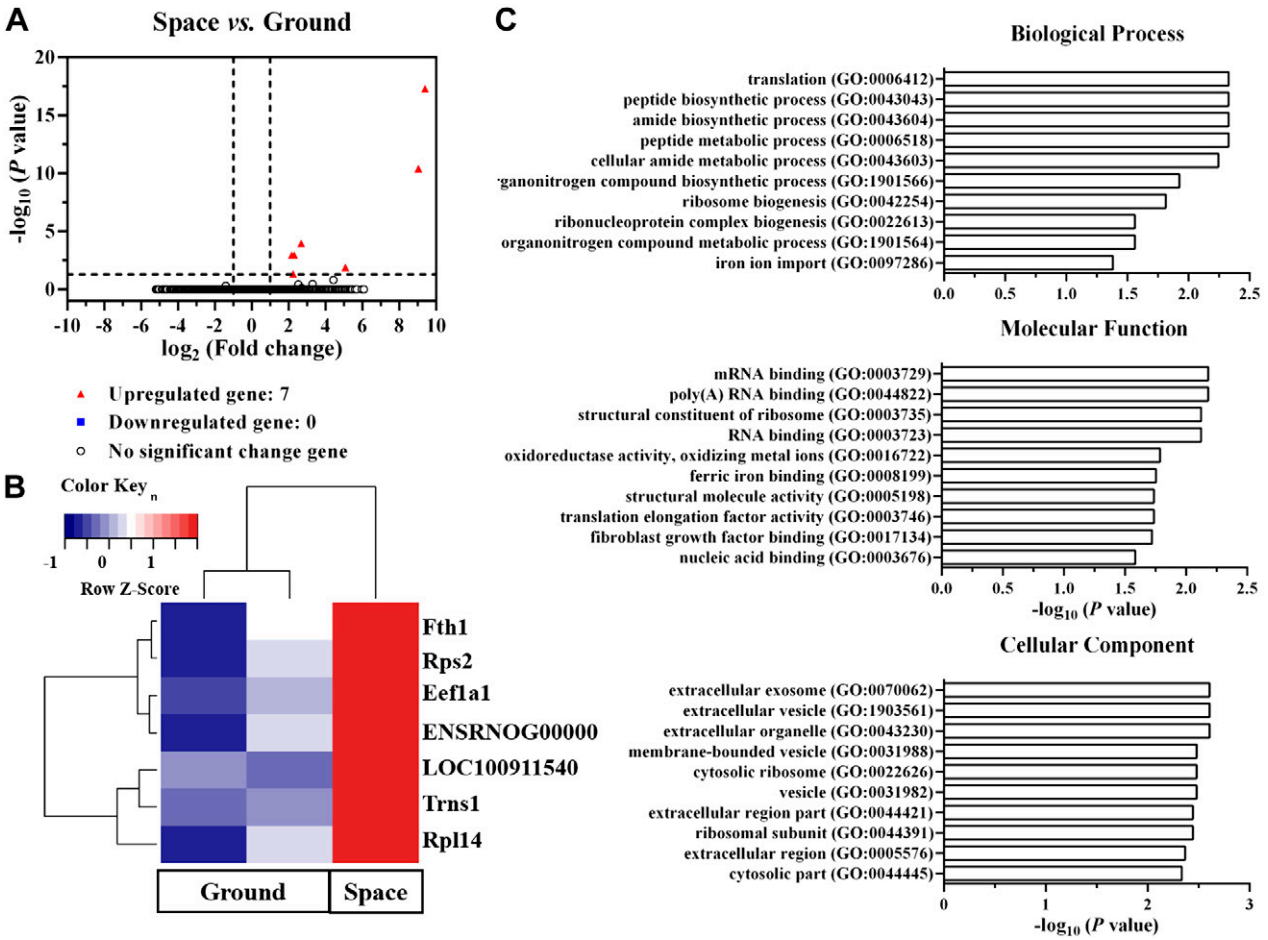

Figure 7. Effects of space microgravity on RNA profile in exosomes collected from the supernatants of rBMSCs cultured for 10 d in space and on the ground. *A*) Volcano plots of exosome RNA profile (space *vs.* ground). The horizontal line represents a *P* value of 0.05, and the 2 vertical lines correspond to 2-fold up or down. The red points represent the up-regulated genes with statistical significance. *B*) Hierarchical clustering analysis of significantly changed genes (space *vs.* ground). The relative abundance of a gene expression in a given sample is colored by its row *z* score, calculated by subtracting the mean expression across all samples from its value for a given sample and then dividing by the SD across all the samples. Each row denotes a gene; the columns represent 1 experiment in space and 2 independent experiments on the ground. *C*) GO term enrichment and pathway analysis of the differentially expressed genes. The top 10 enriched GO terms in biologic process, molecular function, and cellular component were calculated by the value of $-\log_{10}$ (*P* value) and are presented in bar diagrams. Eef1a1, eukaryotic translation elongation factor 1 α 1; ENSRNOG00000058555, miscellaneous RNA with unknown function; Fth1, ferritin heavy chain 1; LOC100911540, pseudogene; poly(A), poly(A) tail; Rpl14, ribosomal protein L14; Rps2, ribosomal protein S2; Trns1, also known as mt-Ts1.

performed to determine the gene enrichment in cellular components, molecular functions, and biologic processes (Fig. 7*C*). It was indicated that these differentially expressed genes are highly enriched in biologic processes such as viral infection, multi-organism cellular process, and biosynthesis, participating in the molecular events of RNA binding, structural constituent of ribosome, oxidoreductase activity, and metal ion oxidization. They are also involved in the cellular components as extracellular exosome, vesicle, and organelle. Together, these data indicated that space microgravity could enhance the mRNA transcription and cell-cell communication among rBMSC-derived differentiated cells.

DISCUSSION

How space microgravity affects the biologic functions of the cells is a key issue from the viewpoint of mechanobiology. This work aims to investigate the hepatogenic potential of rBMSCs in space by directing hepatogenic differentiation *via* biochemical induction and to compare the results with those on the ground. After a 10-d induction in space, the cells presented a more hepatocytelike phenotype than those on the ground, such as 2 nucleoli. Typical biomarker expression of ALB and CK18 and functional testing of lipid droplet production further verified the potential of hepatogenic differentiation and maturation of rBMSC-derived cells. The underlying mechanotransductive mechanisms in space were sophisticated, yielding the distinct expressions of cell adhesion molecule, focal adhesion complexes, and cytoskeletal proteins and enhancing the exosome-mediated mRNA transfer (**Fig. 8**). To our knowledge, this is the first evidence in actual space microgravity to elucidate the biologic features and hepatogenic differentiation of rBMSCs, especially at protein and gene levels.

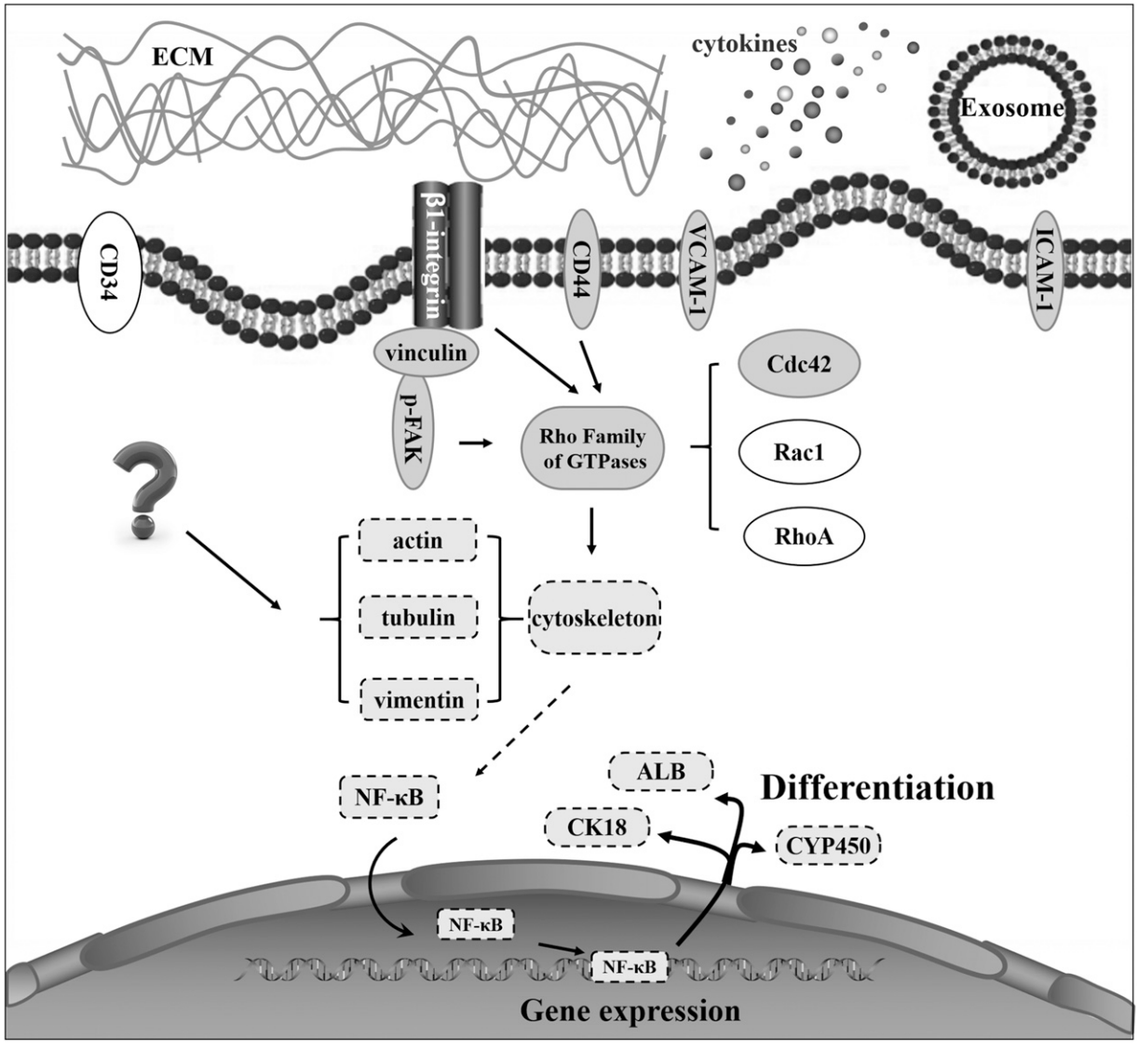

Figure 8. Working model for the effects of space microgravity on hepatogenic differentiation of rBMSCs. Molecules depicted by solid grey boxes (down-regulated), dotted boxes (up-regulated) and solid white boxes (invariant). ECM, extracellular matrix.

Our results conformed to the major findings demonstrated by those studies on rBMSCs or HLCs using clinostats or microgravity effect simulation approaches on the ground, such as decreased cell adhesion molecule expression of ICAM-1 and VCAM-1 (36, 37). Unlike the microgravity effect simulation (12), however, space microgravity could enhance F-actin expression and stress fiber formation (Fig. 5), indicating a different regulating mechanism in rBMSC differentiation between space- and ground-based approaches. It could also provide an appropriate assay for hepatogenic differentiation of rBMSCs, potentially applicable in engineered liver reconstruction as an effective cell source.

Maturation of HLCs derived from MSCs is a key issue for both stem cell biology and potential cell sources in regenerative medicine (38). The most commonly used is a 2-step protocol to direct hepatogenic differentiation, with differentiation medium followed by maturation medium (39–41), or even a 3-step protocol (42, 43), usually taking 20 or even 30 d. This was an extremely long time to differentiate MSCs in space because our spaceflight experiment was performed in the space payload. Evidently, these are not practical for an SJ-10 satellite mission, which only runs in orbit for 12 d. To satisfy this space mission and explore a novel approach in space, a modified 1-step induction protocol (22) was used for directing HLCs with differentiation medium alone. Here, the observed transition of fibroblastlike morphology (Fig. 1) is consistent with the morphologic change in the first step of hepatogenic differentiation (39) even though the specific binucleated cells with small, round, or polygonal shape and platelike structure were not observed. Moreover, differentiated cells in space were strongly positive in, at least, ALB and CK18 staining (Fig. 2) and also presented typical hepatic functions and nucleus features. Taken together, these results allow us to reasonably believe that the cells differentiated from rBMSCs could be more mature in space than on the ground.

In addition to those biochemical factors, the mechanical factors originating from space microgravity could play a

role in directing rBMSCs into HLCs *via* mechanosensation, which is induced by cell adhesion onto the substrate and by force transmission through cytoskeletons (20, 31, 44). In this work, a stem cell phenotype–related adhesive molecule, CD34, maintained the similar expression, but other conventional adhesive molecules of CD44, ICAM-1, and VCAM-1 yieldedreduced expressions in space (Fig. 3). These results suggested that the cells grown in a monolayer in space would not have to attach onto the substrate as closely as on Earth. Because cell adhesion is the initial step for biomechanical and biochemical signaling, it is possible that the difference in ligand availability and structure contributes distinctly to regulate cell adhesion, together with the downstream focal adhesion complexes. Evaluation of 2 typical members of the complexes, β1-integrin and vinculin, presented the opposite manner between in space and on the ground. On one hand, vinculin was down-regulated in space (Fig. 4*E–H*, *N*), implying that the focal adhesions could also be lowered and the ability of cell adherence is then reduced. On the other hand, as a key adhesive molecule in MSCs (45) and hepatocytes (46) in cell adhesion (47), mechanotransduction (48), and liver injury repair (49), β1-integrin expression was enhanced in space (Fig. 4*A–D*, *M*), consistent with those observations from simulated microgravity effect tests (50). Because VCAM-1 expression in space was reduced and fewer β1-integrin–VCAM-1 pairs may be not effective to support cell adhesion, one possible mechanism is that the extra β1-integrins would bind to other ligands to compensate the insufficiency [*e.g.*, collagen I ligand, known to specifically bind to β1-integrin in MSCs in a ground-based study (50)]. This is critical especially for hepatogenic induction of rBMSCs because the reinforced β1-integrin signaling *via* VCAM-1 and/or collagen I binding could potentially favor hepatogenic differentiation (51, 52). Interestingly, actin expression in rBMSCs is higher in space than on the ground (Fig. 5*A–D*, *M*), similar to those observations during parabolic flight at the gene level (19). Tubulin is increased significantly in space compared with ground controls (Fig. 5*E–H*, *N*), also consistent with the observations during parabolic flight (19). Exposure to space microgravity for 3 d leads to a significant increase of vimentin expression (Fig. 5*I–L*, *O*), which is in agreement with previous studies *via* clinostat (19) and, more likely, applied to strengthen the cytoskeletal network *via* vimentin cord, as observed under a varied-gravity vector (20).

The above mechanical signals under space microgravity can also be transduced into biochemical signals *via* mechanosensitive pathways. As typical mechanotransductive molecules, 3 members of Rho GTPase family (Cdc42, Rac1, and RhoA) serve as "molecular switches" and regulate the formation of filopodia, lamellipodia, and stress fibers, respectively, in MSCs (53, 54). Abnormal regulations or functions of the cellular cytoskeleton *via* cell adhesion alter cell phenotype. At the early stage of the directed hepatogenic differentiation of rBMSCs for 3 d under microgravity, β1-integrin expression is up-regulated, but autophosphorylation of adhesion-dependent kinase FAK (Supplemental Fig. S2*A–D*, *Q*) and expressions of Rho GTPases of RhoA (Fig. 6*A–D*, *Q*) and Rac1 (Fig. 6*E–H*, *R*) have no significant differences, and Cdc42 has a slight decline (Fig. 6*I–L*, *S*), as compared with those on the ground. The members of the Rho GTPase family (Cdc42, Rac1, and RhoA) help cells regulate changes in shape by controlling actin dynamics. Generally speaking, RhoA activate ROCK, which in turn inhibits the protein cofilin. Cofilin's function is to reorganize the actin cytoskeleton of a cell; namely, it depolymerizes actin segments (55). Existing literature reported that hepatocyte growth factor was conducive to formation of stress fibers by inhibiting activation of Rho GTPase (56). That explained why our results showed stress fiber was the most obvious at d 3 in space, but Rho GTPase was reduced. Simultaneously, ROCK was dramatically decreased (Fig. 6*M–P*, *T*), but cofilin was also decreased (Supplemental Fig. S3*A–D*, *A*). At the late stage of induced differentiation for 10 d, however, Rac1 and Cdc42 expressions are decreased and phosphorylated-FAK and RhoA expressions are increased dramatically in space compared with ground controls. NF-κB expression is significantly enhanced in space compared with that on the ground at d 3, but the difference between space and ground groups tends to reduce at d 10 (Supplemental Fig. S2*M–P*, *T*). Because hepatogenic differentiation of MSCs in space should result from the coupling of mechanical and chemical signaling, it is reasonably speculated that chemical induction plays major roles at the early stage and mechanical factors work at the late stage. Mechanical and chemical signal molecules translate to cell nucleus–induced changes of nucleoproteins, and their modification in turn affects changes in the cell phenotype (Supplemental Fig. S4). To date, few studies are directed on hepatogenic differentiation of MSCs under space microgravity or ground-based simulation, and further studies are required to isolate the 2 distinct signaling mechanisms.

In summary, this specialized microgravity experiment on an SJ-10 satellite provides an appropriate microenvironment to test the potentials in promoting the differentiation of rBMSCs toward cells with primary hepatic functions. This process is exemplified as the coupling of biochemically induced transdifferentiation of rBMSCs together with mechanotransductive responses in space. Cellular mechanisms and molecular bases of homeostatic and injury-induced liver regeneration are unique and need to be further studied. Nevertheless, utilizing space microgravity to direct hepatogenic differentiation of MSCs could be a novel strategy for obtaining functional HLCs. FJ

ACKNOWLEDGMENTS

The authors thank Lei Zhang, Jianquan Zhang, Zhongfang Deng, Xiang Li, Teng Xie, and Namei Du (Technology and Engineering Center for Space Utilization, Chinese Academy of Sciences) for help in developing hardware and software; Juan Chen and Yuxin Gao (Institute of Mechanics, Chinese Academy of Sciences) for technical support; and Shenbao Chen, Lüwen Zhou, Xiao Zhang, Yuzhen Bi, Bing Shangguan, and Hao Yang (Institute of Mechanics, Chinese Academy of Sciences) for contributions to implement the space experiment. The authors are grateful to the staff members from the National Space Science Center, Chinese Academy of Sciences, and from the China

Academy of Space Technology, China Aerospace Science and Technology Corporation, for contributions to the mission of the SJ-10 Recoverable Scientific Satellite. This work was supported by National Natural Science Foundation of China Grants U1738115 and 31661143044, and Strategic Priority Research Program and Frontier Science Key Project of Chinese Academy of Sciences Grants XDA0402020219, XDA04020416, XDA04073800, and QYZDJSSW-JSC018. The authors declare no conflicts of interest.

AUTHOR CONTRIBUTIONS

D. Lü and M. Long designed research; D. Lü, F. Zhang, and Y. Wu analyzed data; D. Lü, F. Zhang, C. Luo, L. Zheng, N. Li, and C. Zhang performed research; D. Lü and M. Long wrote the manuscript; and S. Sun, C. Wang, and Q. Chen designed and prepared the SCCS hardware.

REFERENCES

1. Zhou, S., Greenberger, J. S., Epperly, M. W., Goff, J. P., Adler, C., Leboff, M. S., and Glowacki, J. (2008) Age-related intrinsic changes in human bone-marrow-derived mesenchymal stem cells and their differentiation to osteoblasts. *Aging Cell* **7**, 335–343
2. Richardson, S. M., Curran, J. M., Chen, R., Vaughan-Thomas, A., Hunt, J. A., Freemont, A. J., and Hoyland, J. A. (2006) The differentiation of bone marrow mesenchymal stem cells into chondrocyte-like cells on poly-L-lactic acid (PLLA) scaffolds. *Biomaterials* **27**, 4069–4078
3. Toma, C., Pittenger, M. F., Cahill, K. S., Byrne, B. J., and Kessler, P. D. (2002) Human mesenchymal stem cells differentiate to a cardiomyocyte phenotype in the adult murine heart. *Circulation* **105**, 93–98
4. Muruganandan, S., Roman, A. A., and Sinal, C. J. (2009) Adipocyte differentiation of bone marrow-derived mesenchymal stem cells: cross talk with the osteoblastogenic program. *Cell. Mol. Life Sci.* **66**, 236–253
5. Oswald, J., Boxberger, S., Jørgensen, B., Feldmann, S., Ehninger, G., Bornhäuser, M., and Werner, C. (2004) Mesenchymal stem cells can be differentiated into endothelial cells in vitro. *Stem Cells* **22**, 377–384
6. Jiang, Y., Jahagirdar, B. N., Reinhardt, R. L., Schwartz, R. E., Keene, C. D., Ortiz-Gonzalez, X. R., Reyes, M., Lenvik, T., Lund, T., Blackstad, M., Du, J., Aldrich, S., Lisberg, A., Low, W. C., Largaespada, D. A., and Verfaillie, C. M. (2002) Pluripotency of mesenchymal stem cells derived from adult marrow. *Nature* **418**, 41–49; erratum: 447, 879–880
7. Aurich, H., Sgodda, M., Kaltwasser, P., Vetter, M., Weise, A., Liehr, T., Brulport, M., Hengstler, J. G., Dollinger, M. M., Fleig, W. E., and Christ, B. (2009) Hepatocyte differentiation of mesenchymal stem cells from human adipose tissue in vitro promotes hepatic integration in vivo. *Gut* **58**, 570–581
8. Sato, Y., Araki, H., Kato, J., Nakamura, K., Kawano, Y., Kobune, M., Sato, T., Miyanishi, K., Takayama, T., Takahashi, M., Takimoto, R., Iyama, S., Matsunaga, T., Ohtani, S., Matsuura, A., Hamada, H., and Niitsu, Y. (2005) Human mesenchymal stem cells xenografted directly to rat liver are differentiated into human hepatocytes without fusion. *Blood* **106**, 756–763
9. Banas, A., Teratani, T., Yamamoto, Y., Tokuhara, M., Takeshita, F., Quinn, G., Okochi, H., and Ochiya, T. (2007) Adipose tissue-derived mesenchymal stem cells as a source of human hepatocytes. *Hepatology* **46**, 219–228
10. Stock, P., Brückner, S., Ebensing, S., Hempel, M., Dollinger, M. M., and Christ, B. (2010) The generation of hepatocytes from mesenchymal stem cells and engraftment into murine liver. *Nat. Protoc.* **5**, 617–627
11. Ratushnyy, A., Ezdakova, M., Yakubets, D., and Buravkova, L. (2018) Angiogenic activity of human adipose-derived mesenchymal stem cells under simulated microgravity. *Stem Cells Dev.* **27**, 831–837
12. Chen, Z., Luo, Q., Lin, C., Kuang, D., and Song, G. (2016) Simulated microgravity inhibits osteogenic differentiation of mesenchymal stem cells via depolymerizing F-actin to impede TAZ nuclear translocation. *Sci. Rep.* **6**, 30322
13. Sheyn, D., Pelled, G., Netanely, D., Domany, E., and Gazit, D. (2010) The effect of simulated microgravity on human mesenchymal stem cells cultured in an osteogenic differentiation system: a bioinformatics study. *Tissue Eng. Part A* **16**, 3403–3412
14. Yin, H., Wang, Y., Sun, Z., Sun, X., Xu, Y., Li, P., Meng, H., Yu, X., Xiao, B., Fan, T., Wang, Y., Xu, W., Wang, A., Guo, Q., Peng, J., and Lu, S. (2016) Induction of mesenchymal stem cell chondrogenic differentiation and functional cartilage microtissue formation for in vivo cartilage regeneration by cartilage extracellular matrix-derived particles. *Acta Biomater.* **33**, 96–109
15. Wang, N., Wang, H., Chen, J., Zhang, X., Xie, J., Li, Z., Ma, J., Wang, W., and Wang, Z. (2014) The simulated microgravity enhances multipotential differentiation capacity of bone marrow mesenchymal stem cells. *Cytotechnology* **66**, 119–131
16. Luna, C., Yew, A. G., and Hsieh, A. H. (2015) Effects of angular frequency during clinorotation on mesenchymal stem cell morphology and migration. *NPJ Microgravity* **1**, 15007
17. Zhang, C., Li, L., Jiang, Y., Wang, C., Geng, B., Wang, Y., Chen, J., Liu, F., Qiu, P., Zhai, G., Chen, P., Quan, R., and Wang, J. (2018) Space microgravity drives transdifferentiation of human bone marrow-derived mesenchymal stem cells from osteogenesis to adipogenesis. *FASEB J.* **32**, 4444–4458
18. Talbot, N. C., Caperna, T. J., and Garrett, W. M. (2013) Growth and Development Symposium: development, characterization, and use of a porcine epiblast-derived liver stem cell line: ARS-PICM-19. *J. Anim. Sci.* **91**, 66–77
19. Aleshcheva, G., Wehland, M., Sahana, J., Bauer, J., Corydon, T. J., Hemmersbach, R., Frett, T., Egli, M., Infanger, M., Grosse, J., and Grimm, D. (2015) Moderate alterations of the cytoskeleton in human chondrocytes after short-term microgravity produced by parabolic flight maneuvers could be prevented by up-regulation of BMP-2 and SOX-9. *FASEB J.* **29**, 2303–2314
20. Zhang, C., Zhou, L., Zhang, F., Lü, D., Li, N., Zheng, L., Xu, Y., Li, Z., Sun, S., and Long, M. (2017) Mechanical remodeling of normally sized mammalian cells under a gravity vector. *FASEB J.* **31**, 802–813
21. Li, Z., Gong, Y., Sun, S., Du, Y., Lü, D., Liu, X., and Long, M. (2013) Differential regulation of stiffness, topography, and dimension of substrates in rat mesenchymal stem cells. *Biomaterials* **34**, 7616–7625
22. Miyazaki, M., Akiyama, I., Sakaguchi, M., Nakashima, E., Okada, M., Kataoka, K., and Huh, N. H. (2002) Improved conditions to induce hepatocytes from rat bone marrow cells in culture. *Biochem. Biophys. Res. Commun.* **298**, 24–30
23. Hu, W. R., Zhao, J. F., Long, M., Zhang, X. W., Liu, Q. S., Hou, M. Y., Kang, Q., Wang, Y. R., Xu, S. H., Kong, W. J., Zhang, H., Wang, S. F., Sun, Y. Q., Hang, H. Y., Huang, Y. P., Cai, W. M., Zhao, Y., Dai, J. W., Zheng, H. Q., Duan, E. K., and Wang, J. F. (2014) Space program SJ-10 of microgravity research. *Microgravity Sci. Technol.* **26**, 159–169
24. Li, N., Wang, C., Sun, S., Zhang, C., Lü, D., Chen, Q., and Long, M. (2018) Microgravity-induced alterations of inflammation-related mechanotransduction in endothelial cells on board SJ-10 satellite. *Front. Physiol.* **9**, 1025
25. Théry, C., Amigorena, S., Raposo, G., and Clayton, A. (2006) Isolation and characterization of exosomes from cell culture supernatants and biological fluids. *Curr. Protoc. Cell Biol.* **30**, 3.22.1–3.22.29
26. Kim, D., Pertea, G., Trapnell, C., Pimentel, H., Kelley, R., and Salzberg, S. L. (2013) TopHat2: accurate alignment of transcriptomes in the presence of insertions, deletions and gene fusions. *Genome Biol.* **14**, R36
27. Mortazavi, A., Williams, B. A., McCue, K., Schaeffer, L., and Wold, B. (2008) Mapping and quantifying mammalian transcriptomes by RNA-Seq. *Nat. Methods* **5**, 621–628
28. Anders, S., and Huber, W. (2010) Differential expression analysis for sequence count data. *Genome Biol.* **11**, R106
29. Ashburner, M., Ball, C. A., Blake, J. A., Botstein, D., Butler, H., Cherry, J. M., Davis, A. P., Dolinski, K., Dwight, S. S., Eppig, J. T., Harris, M. A., Hill, D. P., Issel-Tarver, L., Kasarskis, A., Lewis, S., Matese, J. C., Richardson, J. E., Ringwald, M., Rubin, G. M., and Sherlock, G. (2000) Gene ontology: tool for the unification of biology. The Gene Ontology Consortium. *Nat. Genet.* **25**, 25–29
30. Klaunig, J. E., Goldblatt, P. J., Hinton, D. E., Lipsky, M. M., Chacko, J., and Trump, B. F. (1981) Mouse liver cell culture. I. Hepatocyte isolation. *In Vitro* **17**, 913–925
31. Zhou, L., Zhang, C., Zhang, F., Lü, S., Sun, S., Lü, D., and Long, M. (2018) Theoretical modeling of mechanical homeostasis of a mammalian cell under gravity-directed vector. *Biomech. Model. Mechanobiol.* **17**, 191–203
32. Ban, N., Beckmann, R., Cate, J. H. D., Dinman, J. D., Dragon, F., Ellis, S. R., Lafontaine, D. L. J., Lindahl, L., Liljas, A., Lipton, J. M., McAlear, M. A., Moore, P. B., Noller, H. F., Ortega, J., Panse, V. G.,

Ramakrishnan, V., Spahn, C. M. T., Steitz, T. A., Tchorzewski, M., Tollervey, D., Warren, A. J., Williamson, J. R., Wilson, D., Yonath, A., and Yusupov, M. (2014) A new system for naming ribosomal proteins. *Curr. Opin. Struct. Biol.* **24**, 165–169
33. De la Cruz, J., Karbstein, K., and Woolford, J. L., Jr. (2015) Functions of ribosomal proteins in assembly of eukaryotic ribosomes in vivo. *Annu. Rev. Biochem.* **84**, 93–129
34. Vera, M., Pani, B., Griffiths, L. A., Muchardt, C., Abbott, C. M., Singer, R. H., and Nudler, E. (2014) The translation elongation factor eEF1A1 couples transcription to translation during heat shock response. *eLife* **3**, e03164
35. Liu, H., Ding, J., Chen, F., Fan, B., Gao, N., Yang, Z., and Qi, L. (2010) Increased expression of elongation factor-1α is significantly correlated with poor prognosis of human prostate cancer. *Scand. J. Urol. Nephrol.* **44**, 277–283
36. Grimm, D., Bauer, J., Ulbrich, C., Westphal, K., Wehland, M., Infanger, M., Aleshcheva, G., Pietsch, J., Ghardi, M., Beck, M., El-Saghire, H., de Saint-Georges, L., and Baatout, S. (2010) Different responsiveness of endothelial cells to vascular endothelial growth factor and basic fibroblast growth factor added to culture media under gravity and simulated microgravity. *Tissue Eng. Part A* **16**, 1559–1573
37. Grenon, S. M., Jeanne, M., Aguado-Zuniga, J., Conte, M. S., and Hughes-Fulford, M. (2013) Effects of gravitational mechanical unloading in endothelial cells: association between caveolins, inflammation and adhesion molecules. *Sci. Rep.* **3**, 1494
38. Godoy, P., Schmidt-Heck, W., Natarajan, K., Lucendo-Villarin, B., Szkolnicka, D., Asplund, A., Björquist, P., Widera, A., Stöber, R., Campos, G., Hammad, S., Sachinidis, A., Chaudhari, U., Damm, G., Weiss, T. S., Nüssler, A., Synnergren, J., Edlund, K., Küppers-Munther, B., Hay, D. C., and Hengstler, J. G. (2015) Gene networks and transcription factor motifs defining the differentiation of stem cells into hepatocyte-like cells. *J. Hepatol.* **63**, 934–942; erratum: 64, 525–526
39. Esmaeli, S., Allameh, A., Adelipour, M., Soleimani, M., and Allameh, M. (2017) The impact of oxidative DNA changes and ATM expression on morphological and functional activities on hepatocytes obtained from mesenchymal stem cells. *Biologicals* **47**, 52–58
40. Wu, H. H., Ho, J. H., and Lee, O. K. (2016) Detection of hepatic maturation by Raman spectroscopy in mesenchymal stromal cells undergoing hepatic differentiation. *Stem Cell Res. Ther.* **7**, 6
41. Yan, C., Yang, M., Li, Z., Li, S., Hu, X., Fan, D., Zhang, Y., Wang, J., and Xiong, D. (2014) Suppression of orthotopically implanted hepatocarcinoma in mice by umbilical cord-derived mesenchymal stem cells with sTRAIL gene expression driven by AFP promoter. *Biomaterials* **35**, 3035–3043
42. Cipriano, M., Correia, J. C., Camões, S. P., Oliveira, N. G., Cruz, P., Cruz, H., Castro, M., Ruas, J. L., Santos, J. M., and Miranda, J. P. (2017) The role of epigenetic modifiers in extended cultures of functional hepatocyte-like cells derived from human neonatal mesenchymal stem cells. *Arch. Toxicol.* **91**, 2469–2489
43. Lee, S. W., Min, S. O., Bak, S. Y., Hwang, H. K., and Kim, K. S. (2015) Efficient endodermal induction of human adipose stem cells using various concentrations of Activin A for hepatic differentiation. *Biochem. Biophys. Res. Commun.* **464**, 1178–1184
44. Long, M., Wang, Y. R., Zheng, H. Q., Shang, P., Duan, E. K., and Lu, D. Y. (2015) Mechano-biological coupling of cellular responses to microgravity. *Microgravity Sci. Technol.* **27**, 505–514
45. Song, K., Huang, M., Shi, Q., Du, T., and Cao, Y. (2014) Cultivation and identification of rat bone marrow-derived mesenchymal stem cells. *Mol. Med. Rep.* **10**, 755–760
46. Speicher, T., Siegenthaler, B., Bogorad, R. L., Ruppert, R., Petzold, T., Padrissa-Altes, S., Bachofner, M., Anderson, D. G., Koteliansky, V., Fässler, R., and Werner, S. (2014) Knockdown and knockout of β1-integrin in hepatocytes impairs liver regeneration through inhibition of growth factor signalling. *Nat. Commun.* **5**, 3862
47. Lee, J. W., Kim, Y. H., Park, K. D., Jee, K. S., Shin, J. W., and Hahn, S. B. (2004) Importance of integrin beta1-mediated cell adhesion on biodegradable polymers under serum depletion in mesenchymal stem cells and chondrocytes. *Biomaterials* **25**, 1901–1909
48. Ode, A., Kopf, J., Kurtz, A., Schmidt-Bleek, K., Schrade, P., Kolar, P., Buttgereit, F., Lehmann, K., Hutmacher, D. W., Duda, G. N., and Kasper, G. (2011) CD73 and CD29 concurrently mediate the mechanically induced decrease of migratory capacity of mesenchymal stromal cells. *Eur. Cell. Mater.* **22**, 26–42
49. Aldridge, V., Garg, A., Davies, N., Bartlett, D. C., Youster, J., Beard, H., Kavanagh, D. P., Kalia, N., Frampton, J., Lalor, P. F., and Newsome, P. N. (2012) Human mesenchymal stem cells are recruited to injured liver in a β1-integrin and CD44 dependent manner. *Hepatology* **56**, 1063–1073
50. Meyers, V. E., Zayzafoon, M., Gonda, S. R., Gathings, W. E., and McDonald, J. M. (2004) Modeled microgravity disrupts collagen I/integrin signaling during osteoblastic differentiation of human mesenchymal stem cells. *J. Cell. Biochem.* **93**, 697–707
51. Popov, C., Radic, T., Haasters, F., Prall, W. C., Aszodi, A., Gullberg, D., Schieker, M., and Docheva, D. (2011) Integrins α2β1 and α11β1 regulate the survival of mesenchymal stem cells on collagen I. *Cell Death Dis.* **2**, e186
52. Bi, H., Ming, L., Cheng, R., Luo, H., Zhang, Y., and Jin, Y. (2017) Liver extracellular matrix promotes BM-MSCs hepatic differentiation and reversal of liver fibrosis through activation of integrin pathway. *J. Tissue Eng. Regen. Med.* **11**, 2685–2698
53. Meyers, V. E., Zayzafoon, M., Douglas, J. T., and McDonald, J. M. (2005) RhoA and cytoskeletal disruption mediate reduced osteoblastogenesis and enhanced adipogenesis of human mesenchymal stem cells in modeled microgravity. *J. Bone Miner. Res.* **20**, 1858–1866
54. Zayzafoon, M., Meyers, V. E., and McDonald, J. M. (2005) Microgravity: the immune response and bone. *Immunol. Rev.* **208**, 267–280
55. Kiss, C., Li, J., Szeles, A., Gizatullin, R. Z., Kashuba, V. I., Lushnikova, T., Protopopov, A. I., Kelve, M., Kiss, H., Kholodnyuk, I. D., Imreh, S., Klein, G., and Zabarovsky, E. R. (1997) Assignment of the ARHA and GPX1 genes to human chromosome bands 3p21.3 by in situ hybridization and with somatic cell hybrids. *Cytogenet. Cell Genet.* **79**, 228–230
56. Birukova, A. A., Alekseeva, E., Mikaelyan, A., and Birukov, K. G. (2007) HGF attenuates thrombin-induced endothelial permeability by Tiam1-mediated activation of the Rac pathway and by Tiam1/Rac-dependent inhibition of the Rho pathway. *FASEB J.* **21**, 2776–2786
57. Dittmer, T. A., and Misteli, T. (2011) The lamin protein family. *Genome Biol.* **12**, 222
58. Herrmann, H., and Aebi, U. (2016) Intermediate filaments: structure and assembly. *Cold Spring Harb. Perspect. Biol.* **8**, a018242
59. Rønningen, T., Shah, A., Oldenburg, A. R., Vekterud, K., Delbarre, E., Moskaug, J. Ø., and Collas, P. (2015) Prepatterning of differentiation-driven nuclear lamin A/C-associated chromatin domains by GlcNAcylated histone H2B. *Genome Res.* **25**, 1825–1835

Received for publication October 1, 2018.
Accepted for publication November 12, 2018.